Hydrodynamic performance of an array of Wave Energy Converters in front of a vertical wall

Eva Loukogeorgaki and Ioannis K. Chatjigeorgiou

Abstract—**In this paper, the hydrodynamic performance (hydrodynamic behaviour and power absorption) of a linear array of nine, free-floating heaving Wave Energy Converters (WECs), placed in front of a bottom-mounted, finite–length, vertical wall of negligible thickness, is investigated numerically in the frequency domain under the action of regular waves. The corresponding diffraction/radiation problem is solved by utilizing the conventional Boundary Integral Equation method. Initially, we examine and discuss the limitations of the widely used method of images along with the assumption of a "pure" wave reflecting wall of infinite length on the calculation of the WECs' exciting forces. Next, we investigate the effect of the array's distance from the wall on the physical quantities describing the performance of the array. The results illustrate that the infinite wall assumption leads to an under-estimation of the WECs' heave exciting forces at quite small wave numbers, even for the case of the lengthy wall considered in this paper. The distance of the array from the wall affects significantly the array's performance, mainly, in the low frequency range. The decrease of the aforementioned distance leads to a great reduction of the WECs' heave response in the wave number range, where resonance occurs, as a result of the corresponding decrease of the heave forces. Compared to the isolated array, the presence of the wall enhances constructive interactions among the WECs and it increases the array's absorbed power efficiency at specific wave number ranges, depending upon the array's distance from the wall.**

Keywords—**Array of wave energy converters, hydrodynamic interactions, vertical wall, wave energy.**

I. Introduction

WAVE energy presents globally an inexhaustible energy source. Its effective and economically efficient exploitation can contribute to the reduction of greenhouse gas emissions and, therefore, to the efficient mitigation of climate change effects, while, at the same time, it can support a long-term economic growth of offshore and coastal areas [1]. Currently, the wave energy sector is continuously developing and up to now different types of Wave Energy Converters (WECs), in terms of power absorption mechanism, have been designed and developed (e.g., [2]), aiming at delivering commercially competitive solutions.

Irrespectively of the selected WEC's type, it is clear that for absorbing a significant amount of wave power the deployment of multiple WECs arranged in arrays is required. These arrays can be installed and operate in offshore areas, where waves of higher energy content can be exploited, or at near-shore locations, with the potential to overcome specific drawbacks (e.g. survivability issues) and reduce construction and operation/maintenance costs. In near-shore sites, within the framework of integrating WEC technologies with other marine facilities (e.g., [3]-[4]), cost-efficient solutions can be also realized by installing WECs arrays in front of existing coastal structures, such as vertical (wall-type) breakwaters. In those cases, hydrodynamic interactions between the WECs and the breakwater are additionally introduced, which may have a direct effect on the absorbed power and, generally, on the overall performance of the array.

Considering the case of a *single* floating body in front of a bottom-mounted vertical wall, the relevant diffraction and radiation problem for a truncated free-floating cylinder has been investigated in the frequency domain in [5] and [6] respectively. In [7], the power absorption of a single heaving WEC placed in front of a wall has been numerically examined and assessed under the action of regular and irregular waves of various wave directions, for different shapes (cone and spherical cylinder), sizes and drafts of the WEC, as well as for different distances of the WEC from the wall. In all the above studies, the wall is taken into account by utilizing the method of images, where the hydrodynamic problem is solved for the floating body and its image (virtual body) with respect to the wall, without the presence of the bottom-mounded, vertical boundary. The method is completed by considering the simultaneous action of the actual incident wave train propagating, say, at angle β with respect to the horizontal, and the "pure" reflected wave train propagating at angle $180^o - \beta$. It is straightforward that the method of images assumes

Paper ID number: 1464
Thematic track: Wave hydrodynamic modelling
E. Loukogeorgaki is Assistant Professor at the Department of Civil Engineering, Aristotle University of Thessaloniki, Thessaloniki, 54124, Greece (e-mail: eloukog@civil.auth.gr).
I.K. Chatjigeorgiou is Professor at the School of Naval Architecture and Marine Engineering, National Technical University of Athens, Athens, 15773, Greece (e-mail: chatzi@naval.ntua.gr).

immediately, and unavoidably a "pure" wave reflecting wall of infinite extent, which, although enables the realization of positive effects in terms of power absorption [8], it does not represent the real physical problem of many practical applications. Except of the above, two-dimensional approximations have been used in [9] to describe resonant behaviour of a free-floating half-immersed cylinder in the presence of a vertical rigid wall.

As for the case of an *array* of WECs in front of breakwaters, the power absorption of an array of surge oscillating WECs in front of π–shaped "pure" reflecting harbour walls has been studied in [10]. Mavrakos et al. [11] investigated and assessed in both frequency and time domain the power absorption of an array of five heaving WECs in front of a fixed-bottom vertical wall. The interaction of the WECs with the wall has been modelled by utilizing again the method of images. Recently, the performance of an array of heaving WECs in front of a box-type breakwater of infinite length has been studied analytically in [12], while the case of nine, free-floating heaving WECs placed in front of a fixed rectangular pontoon of finite length has been investigated in the frequency domain in [13], emphasizing on the effect of various geometrical parameters (e.g., dimensions of the pontoon, distance of the array from the pontoon etc.) and of the Power Take Off (PTO) characteristics on the array's and the individual WEC's interaction factors.

The present paper focuses on the numerical investigation of the performance (hydrodynamic behaviour and power absorption) of a linear array of WECs placed in front of a bottom-mounted vertical wall. The wall is considered to have finite length and negligible thickness, while the array consists of a sufficient number of free-floating heaving WECs of cylindrical cross-section. Each WEC is assumed to absorb power through a linear PTO mechanism, actuated from the heave motion of each WEC. The numerical analysis is implemented in the frequency domain under the action of perpendicular to the wall regular waves. The corresponding diffraction/radiation problem, including hydrodynamic interactions among the WECs and between the wall and the WECs, is solved by utilizing the conventional Boundary Integral Equation (BIE) method. Initially, exciting forces for finite- and infinite-length wall cases are compared in order to examine and reveal the limitations of the widely used method of images along with the assumption of a "pure" wave reflecting wall. The latter case is formulated and solved using the matched eigenfunction expansion technique and the "direct" solution methodology for the numerical implementation [14]-[15]. Next, for the finite-length wall, we investigate the effect of the distance between the WECs and the wall on the excitation forces, the response and the power absorption of the array. Results are, also, compared with the case of an isolated array for demonstrating more clearly the effect of the existence of the wall on the performance of the array. Finally, for all cases examined, constructive and destructive interactions in terms of the array's absorbed power are quantified and examined.

II. NUMERICAL MODELLING

A linear array of N mutually interacting, free-floating heaving WECs are placed in an area of finite and constant water depth h in front of a bottom–mounted, vertical wall of finite length l_w and of negligible thickness (Fig. 1). Each WECj, $j = 1, \dots, N$, has cylindrical cross-section of radius b and of draft h_1, as shown in Fig. 1b, where the PTO mechanism is schematically represented as a linear damping system, with damping coefficient b_{ptoj}, $j = 1, \dots, N$. The WECs are distributed uniformly in the array having a centre–to–centre spacing equal to l_b, while all WECs are placed at a distance c from the wall (Fig. 1). The array and the wall are subjected to the action of regular incident waves of linear amplitude A and of circular frequency ω that propagate at angle β with respect to the global horizontal X axis.

The hydrodynamic analysis of the WECs array, including hydrodynamic interaction effects among the WECs and between the wall and the WECs, is performed in the frequency domain and it relies on the BIE method, which is numerically realized using the WAMIT© software [16]. The analysis is based on a three-dimensional linear potential theory, where each WEC is also assumed to oscillate freely only along the WEC's working direction, i.e., along the vertical z axis (Fig. 1b). Therefore, for each WECj, $j = 1, \dots, N$, all degrees of freedom, except the one corresponding to heave, are considered ideally restricted. Assuming inviscid and incompressible fluid with irrotational flow, the velocity potential is introduced for describing the fluid motion. Its complex spatial part is given by the following equations [16]-[17]:

$$\Phi = \underbrace{(\Phi_I + \Phi_S)}_{\Phi_D} + i\omega \sum_{j=1}^{N} \xi_3^j \Phi_j \tag{1}$$

$$\Phi_I = \frac{igA}{\omega} \frac{cosh[k_0(Z+h)]}{cosh(k_0 h)} e^{-ik_0(Xcos\beta + Ysin\beta)} \tag{2}$$

where, Φ_I is the incident wave potential, Φ_S is the scattered potential, associated with the scattered disturbance of the incident waves from all WECs and the wall, Φ_D is the diffraction potential, Φ_j, $j = 1, \dots, N$, are the radiation potentials, related to the waves radiated from all WECs due to their forced motion in heave, ξ_3^j, $j = 1, \dots, N$, are the complex amplitudes of the WECs' heave motions, g is the gravitational acceleration and k_0 is the wave number.

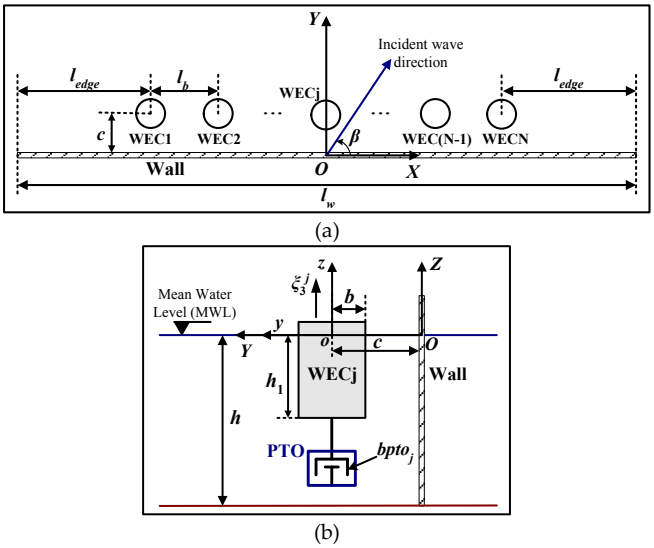

Fig. 1. Geometry of the examined problem and definition of basic quantities: $X-Y$ (a) and $Y-Z$ (b) plane. $OXYZ$ is the global coordinate system, while $oxyz$ presents the local coordinate system of each WEC.

The potentials Φ_m ($m = D$ or $m = j$) satisfy the Laplace equation everywhere in the fluid domain, while, additionally, they are subjected to the following linearized boundary conditions on the free surface (3), the sea bottom (4) and the bodies (5-6) [16]-[17], in order to form the 1st order boundary value problem:

$$\frac{\partial \Phi_m}{\partial Z} - \frac{\omega^2}{g}\Phi_m = 0 \quad \text{on} \quad Z = 0 \tag{3}$$

$$\frac{\partial \Phi_m}{\partial Z} = 0 \quad \text{on} \quad Z = -h \tag{4}$$

$$\frac{\partial \Phi_D}{\partial n} = 0 \tag{5}$$

$$\frac{\partial \Phi_j}{\partial n} = n_3^j \quad \text{for} \quad j = 1, \dots, N \tag{6}$$

In (6), which is applied only to the wetted surface of the WECs, n_3^j is the normal unit vector of WECj along z.

The boundary integral equations for the unknown diffraction and radiation potentials on the boundary of all the bodies (WECs and wall) and of the WECs respectively are formed by utilizing Green's theorem. The corresponding boundary value problem is, then, solved based on a three dimensional low-order panel method [16]-[17]. Since a wall of negligible thickness is taken into account, zero-thickness dipole panels [17] are used for modelling its wetted surface.

Having solved the 1st order boundary value problem, the heave exciting force, F_Z^i, $i = 1, \dots, N$, applied on each WECi, the added mass, A_{ij}, and radiation damping, B_{ij} coefficients are calculated as follows:

$$F_Z^i = -i\omega\rho \iint_{S_B^i} n_3^i \Phi_D ds\,, \qquad i = 1, \dots, N \tag{7}$$

$$A_{ij} - \frac{i}{\omega} B_{ij} = \rho \iint_{S_B^i} n_3^i \Phi_j ds\,, \quad i,j = 1, \dots, N \tag{8}$$

where S_B^i is the wetted surface of the i^{th} WEC and ρ is the water density.

The amplitudes of the WECs' heave motions, ξ_3^j, $j = 1, \dots, N$, are, then, obtained from the solution of the following linear system of equations:

$$\sum_{j=1}^{N} \left[-\omega^2\left(M_{ij} + A_{ij}\right) + i\omega\left(B_{ij} + B_{ij}^{PTO}\right) + C_{ij}\right]\xi_3^j = F_3^i \quad i = 1, \dots, N \tag{9}$$

In (9), M_{ij} and C_{ij} are the mass matrix and hydrostatic - gravitational stiffness coefficients respectively, while, B_{ij}^{PTO} represents the damping coefficients that originate from the PTO mechanism. In the present paper, for each WECj, $j = 1, \dots, N$, this mechanism is modelled as a linear damping system (Fig. 1a), with damping coefficient b_{PTOj}, actuated from the heave motion of the corresponding WEC. Thus, in (9) $B_{ij}^{PTO} = b_{PTOj}$ for $i = j = 1, \dots, N$, while $B_{ij}^{PTO} = 0$ for $i \neq j$.

The heave response of each WEC is expressed in terms of the Response Amplitude Operator (10):

$$RAO_3^j = \frac{\left|\xi_3^j\right|}{A} \tag{10}$$

where $\left|\xi_3^j\right|$ is the amplitude of the complex quantity ξ_3^j.

The mean power, $p(\omega)$, absorbed by the whole array at a specific ω is calculated as follows:

$$p(\omega) = \sum_{j=1}^{N} p_j(\omega) \tag{11}$$

where $p_j(\omega)$, $j = 1, \dots, N$, is the power absorbed by WECj, calculated using (12):

$$p_j(\omega) = 0.5 b_{PTOj} \omega^2 \left|\xi_3^j\right|^2 \tag{12}$$

Moreover, the existence of positive or negative effects of the WECs' hydrodynamic interactions on the array's absorbed power is appropriately quantified by utilizing the modified interaction factor $q_{mod}(\omega)$, as introduced by [18]. For a given ω, this factor is defined as the ratio of the difference between the power absorbed by the N WECs of the array minus the power absorbed by the same number of isolated WECs (no consideration of hydrodynamic interactions), divided by the maximum (among the examined ω values) power absorbed by N isolated WECs. That is [18]-[19]:

$$q_{mod}(\omega) = \frac{p(\omega) - Np_{iso}(\omega)}{Nmaxp_{iso}(\omega)} \quad (13)$$

In (13), $p_{iso}(\omega)$ corresponds to the power absorbed by an isolated WEC at the examined ω, while $maxp_{iso}(\omega)$ is the maximum (among the examined ω values) power absorbed by this WEC. Positive and negative values of $q_{mod}(\omega)$ denote respectively constructive and destructive interactions in terms of power absorption.

Finally, for revealing the limitations of the infinite wall assumption, the diffraction problem for the case of an array situated in front of a "pure" wave–reflecting wall of infinite length ($l_w \to \infty$) is formulated and solved. This is achieved by utilizing the method of images (e.g., [11]), along with semi-analytical considerations of the relevant hydrodynamic boundary value problem based on the matched eigenfunction expansion technique and the "direct" solution methodology for the numerical implementation. More details can be found in [14]-[15].

III. Characteristics of the Problem Examined

The BIE-based numerical model described above is applied for the case of an array of $N = 9$ WECs (Fig. 1a) of radius $b = 1.0$ m, non–dimensional draft $h_1/b = 1.0$ and mass equal to 3,220.13 kgr. All WECs in the array are considered to have the same PTO characteristics; namely, $B_{ij}^{PTO} = b_{PTO}$, $i = j = 1, \ldots, N$. According to [20], the b_{PTO} value is taken equal to the heave radiation damping of an isolated WEC at its heave natural frequency, ω_{n3}^{iso}, i.e., $b_{PTO} = B_{33}^{iso}(\omega = \omega_{n3}^{iso})$. Based on the hydrodynamic analysis of an isolated WEC, ω_{n3}^{iso} has been calculated equal to 2.525 rad/s (non-dimensional wave number $k_0 b = 0.65$), leading to $b_{PTO} = 826.099$ Nm/s.

The WECs are placed in front of a wall of non-dimensional length $l_w/b = 72$ and are distributed uniformly within the array with non–dimensional centre–to–centre spacing equal to $l_b/b = 4$ ($l_{edge}/b = 20$, with l_{edge} denoting the distance between the centres of the two outer WECs in the array with the corresponding edges of the wall, Fig. 1a). Two different values of non-dimensional WECs' distance from the wall, c/b, are investigated, equal to 2 and 4. The array and the wall are placed in an area of non–dimensional depth $h/b = 10$ and they are subjected to regular incident waves of direction $\beta = 270$ deg (Fig. 1a) with non–dimensional wave number varying between 0.01 and 4.0.

IV. Results and Discussion

In the following sections the results of the present investigation are presented and discussed. Initially, for an array with $c/b = 4$, the exciting forces applied on the WECs are compared for finite- and infinite-length wall cases to reveal the limitations of the infinite wall concept. Next, extended results are presented for the finite-length wall focusing on the effect of c/b on the physical quantities describing the hydrodynamic performance of the array. Results for an isolated array (i.e., $l_w/b = 0$) are also cited for illustrating more clearly the effect of the presence of the wall on the performance of the array. It is noted that the symmetry of the array with respect to the examined incident wave direction leads to the same exiting forces and responses for WECi and WECj, with: (a) $i = 1$ and $j = 9$, (b) $i = 2$ and $j = 8$, (c) $i = 3$ and $j = 7$ and (d) $i = 4$ and $j = 6$.

A. WECs' exciting forces for finite- and infinite-length wall cases

In Figs. 2-4, the exciting forces applied on WECj, $j = 1, 3, 5, 7$ and 9, for the finite-length wall are compared with the corresponding ones obtained analytically assuming $l_w \to \infty$. Except of the heave exciting forces, F_Z, comparison is also made in terms of the surge, F_X, and the sway, F_Y, forces. The latter forces are presented normalized by $\rho g A b^2$, while the heave forces have been normalized by $\rho g A \pi b^2$.

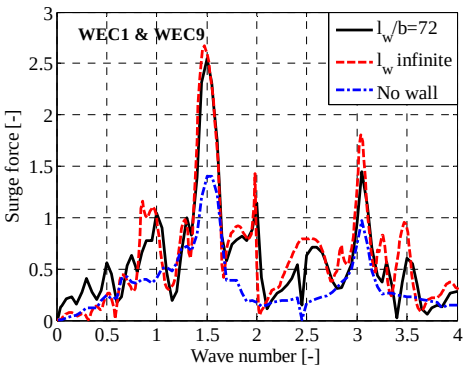

(a)

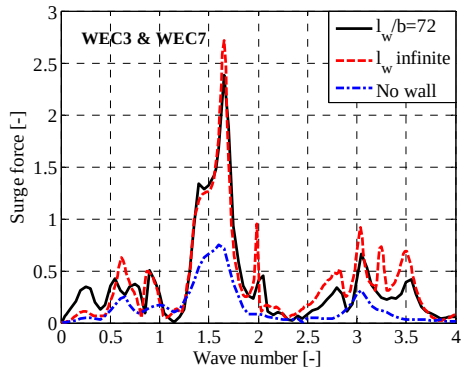

(b)

Fig. 2. Comparison of the surge force, F_X, applied on WEC1 & WEC9 (a) and WEC3 & WEC7 (b) for $l_w/b = 72$ ($c/b = 4$), $l_w/b \to \infty$ ($c/b = 4$) and $l_w/b = 0$ (no wall).

Regarding the surge forces (Fig. 2), F_X for WECj, $j = 1, 3, 7$ and 9 have non-zero values attributed to the hydrodynamic interactions among the WECs and between the wall and the WECs (the same holds true for F_X for WECj, $j = 2, 4, 6$ and 8, not shown here due to space constraints), while F_X for WEC5 is cancelled due to the symmetry of the array with respect to $\beta = 270°$. For both $l_w/b = 72$ and $l_w \to \infty$, F_X for all WECj, $j = 1, 3, 7$ and 9 varies intensively relative to the non-dimensional wave number, $k_0 b$, having an irregular variation pattern

with multiple sharp peaks and successive local minima. The F_X results for $l_w \to \infty$ agree quite well with the ones obtained for $l_w/b = 72$, since the latter case corresponds to a lengthy wall with large outer WEC's centre–to–wall's edge distance ($l_{edge}/b = 20$). It is emphasized, however, that differences among these two cases do exist and, therefore, the infinite wall assumption realized numerically by the method of images should be used with absolute care.

Continuing with the sway exciting forces (Fig. 3), F_Y for WECj, $j = 1, 3, 5, 7$ and 9 and for both l_w cases considered, shows, contrary to the case of the isolated array, an intense variation pattern, characterized by the existence of successive peaks at k_0b~0.4, 1.1, 2.0, 2.8 and 3.5 respectively, with successively decreasing values towards higher frequencies (the same holds true for F_Y for WECj, $j = 2, 4, 6$ and 8, not shown here due to space constraints). Moreover, the transition from the outer WECs (WECj, $j = 1$ and 9, Fig. 3a) to the inner WECs (WECj, $j = 3$ and 7, Fig. 3b) and, finally, to the middle WEC (WEC5, Fig. 3c) leads to the existence of one additional local maximum at k_0b~1.7. Compared to $l_w/b = 72$, the infinite wall assumption does not lead to significant differences of the sway forces even for the outer WECs, due to their large distance from the corresponding wall edges.

With regard to the heave exciting forces (Fig. 4), F_Z for all WECs considered and for both $l_w/b = 72$ and $l_w \to \infty$ have significant values at $0.01 \le k_0b \le 1.0$, while at $k_0b > 1.0$ F_Z becomes practically equal to zero. For $l_w \to \infty$, F_Z decreases quite rapidly from the maximum value of 2 (at $k_0b = 0.01$) up to k_0b~0.35, where it exhibits a local minimum, with value almost equal to zero. An increase of F_Z follows leading to non–zero heave forces up to $k_0b = 1.0$. It is interesting to note that the existence of a maximum F_Z value equal to 2 at $k_0b = 0.01$ is attributed to the assumption of "pure" wave reflection by the infinite–length wall. However, this is not observed for $l_w/b = 72$, where a finite–length wall has been considered, as in the case of real-world applications. More specifically, for the examined finite-length wall case, F_Z starts its variation from ~1.1 (at $k_0b = 0.01$), which is close to the limiting value of 1 as exists in the case of the isolated array, and it, then, increases rapidly up to k_0b~0.05, where the F_Z peak (global maximum) occurs. This in turn leads to larger F_Z values, especially at $0.03 \le k_0b < 0.1$, for WECj, $j = 1, 3, 5, 7$ and 9 compared to $l_w \to \infty$. For the rest examined k_0b range the variation of F_Z for each WECj, $j = 1, 3, 5, 7$ and 9 is analogous with the variation of the corresponding heave exciting force obtained for the infinite-length wall case. Analogous conclusions can be drawn for the heave force of WECj, $j = 2, 4, 6$ and 8 (relevant results are not included here due to space constraints).

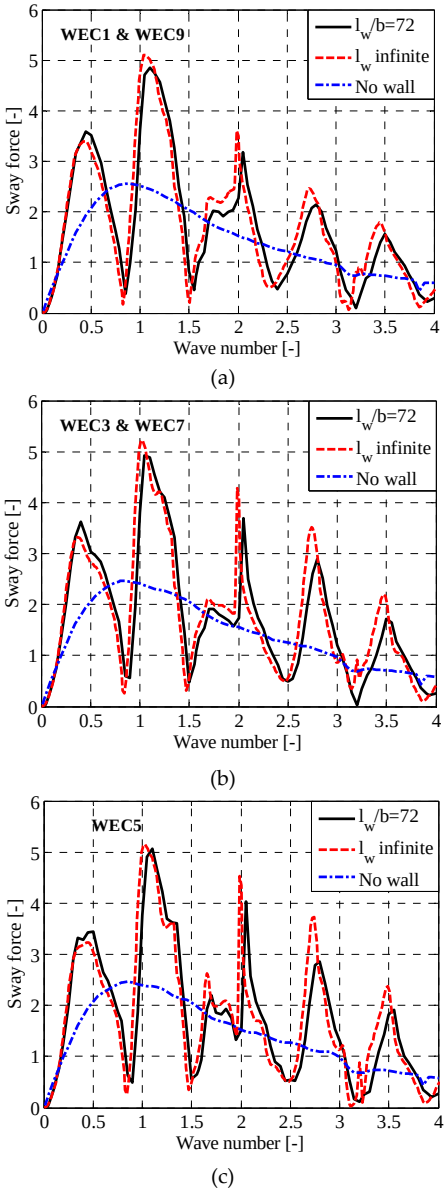

Fig. 3. Comparison of the sway force, F_Y, applied on WEC1 & WEC9 (a), WEC3 & WEC7 (b) and WEC5 (c) for $l_w/b = 72$ ($c/b = 4$), $l_w/b \to \infty$ ($c/b = 4$) and $l_w/b = 0$ (no wall).

Concluding, it can be stated that the infinite wall assumption has limitations regarding the accurate estimation of the WECs' heave exciting forces in the low frequency range, even when a wall of large length (with large outer WEC's center–to–wall's edge distances) is taken into account, since the consideration of a "pure" wave–reflecting wall of infinite length leads to under-estimation of the aforementioned physical quantities. This assumption seems not to have a significant effect on the WECs' surge and sway forces for the finite l_w case examined in the present paper. However, differences between finite- and infinite-length wall do exist; hence, the infinite wall assumption realized numerically by the method of images should be carefully used.

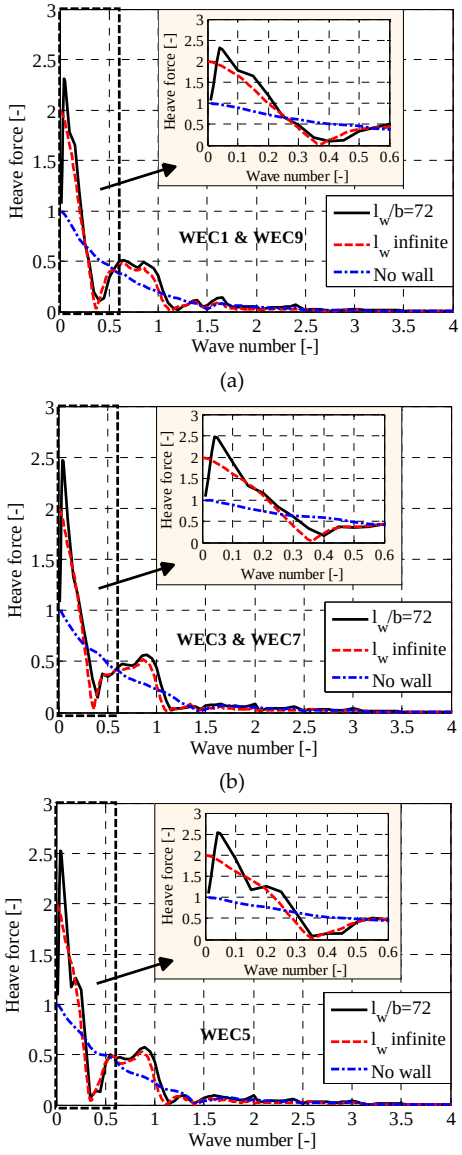

Fig. 4. Comparison of the heave force, F_Z, applied on WEC1 & WEC9 (a), WEC3 & WEC7 (b) and WEC5 (c) for $l_w/b = 72$ ($c/b = 4$), $l_w/b \to \infty$ ($c/b = 4$) and $l_w/b = 0$ (no wall).

B. *Effect of WECs-wall distance on the exciting forces*

The effect of WECs-wall distance, c/b, on the exciting forces applied on the WECs is shown in Figs. 5-7. Except of the heave exciting forces, F_Z, (Figs. 6-7), results for the surge, F_X (Fig. 5a), and the sway, F_Y (Figs. 5b-5c), forces are also presented indicatively for the outer (WECj, $j = 1$ and 9) and the middle (WEC5) devices of the array.

Starting with the surge forces (Fig. 5a), for both examined c/b values, the variation of F_X for each WEC follows a profound irregular pattern. By increasing the distance of the array from the wall, F_X varies more intensively, having a larger number of sharp maxima and local minima and a bit larger values at specific k_0b ranges compared to $c/b = 2$. Compared to the isolated array, it is clear that the presence of the wall, irrespectively of the c/b value examined, leads to a more intense variation and larger values of F_X, attributed to wall-edge effects.

In the case of the sway forces (Figs. 5b-5c), F_Y for $c/b = 2$ and for each WECj, $j = 1, 5$ and 9, shows, contrary to the case of the isolated array, an intense variation pattern, characterized by the existence of three successive peaks at k_0b~0.7, 2.2 and 3.5 respectively, with successively decreasing values towards larger k_0b values. By increasing the array's distance from the wall, F_Y varies more intensively, having a larger number of distinctive successive local maxima (at k_0b~0.4, 1.1, 2.0, 2.8 and 3.5 respectively). The above difference leads in turn to smaller F_Y values for $c/b = 4$ at $0.5 < k_0b < 1.0$ and $2.1 < k_0b < 2.7$ compared to the case of $c/b = 2$.

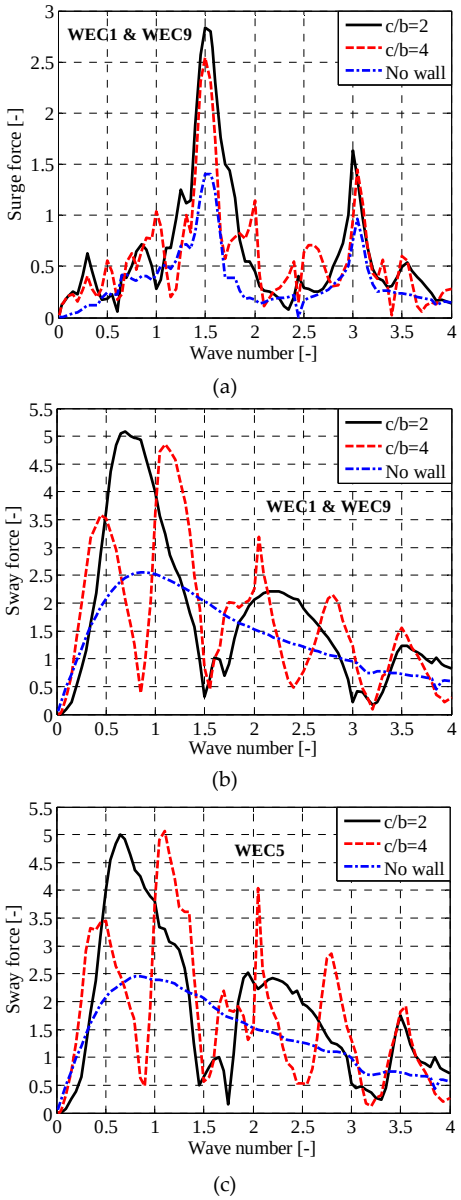

Fig. 5. Effect of c/b on surge force, F_X, applied on WEC1 & WEC9 (a), and sway force, F_Y, applied on WEC1 & WEC9 (b) and WEC5 (c).

Regarding the heave exciting forces (Figs. 6-7), for all WECs of the array and for $c/b = 4$, the variation of F_Z begins from the value of ~1.1 at $k_0b = 0.01$ and it is characterized by a rapid increase up to k_0b~0.05, where the peak of F_Z (global maximum) occurs. Then, F_Z decreases quite rapidly up to k_0b~0.35, where it obtains a

1st local minimum, with value close to zero. Finally, an increase of F_Z follows leading to non–zero heave forces at $0.35 < k_0b \leq 1.0$. Analogous variation pattern is observed for $c/b = 2$. However, the decrease of the array's distance from the wall leads to: (a) the occurrence of a second (local) maximum value at k_0b~0.25, which is more pronounced for the inner (i.e., WEC4 and WEC6, Fig. 7a) and the middle (WEC5, Fig. 7b) devices of the array and (b) a shift of the 1st F_Z local minimum at a larger k_0b value approximately equal to 0.75. This in turn leads to larger F_Z values for $c/b = 2$ at $0.2 < k_0b < 0.5$ compared to $c/b = 4$, while the opposite holds true at $0.5 < k_0b < 1.0$.

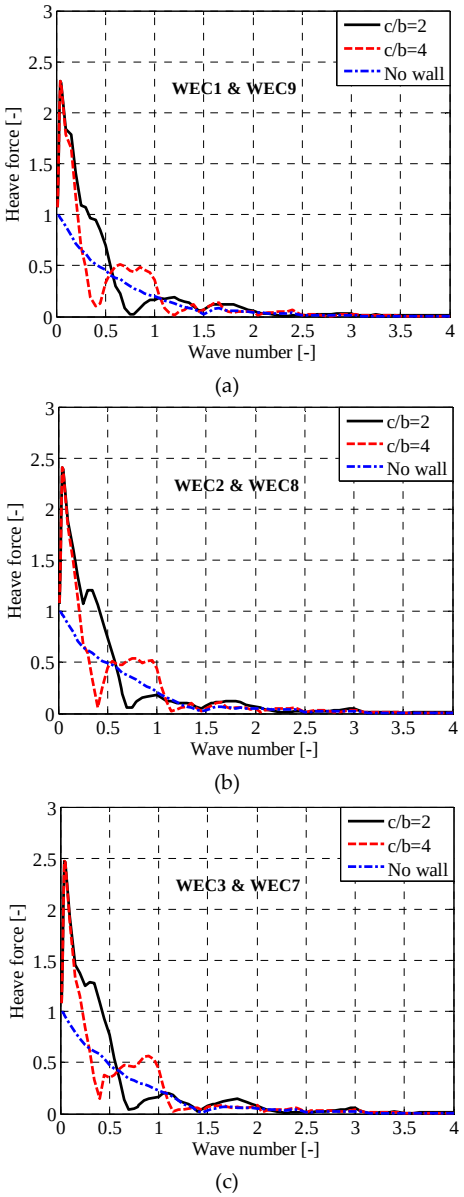

Fig. 6. Effect of c/b on heave force, F_Z, applied on WEC1 & WEC9 (a), WEC2 & WEC8 (b) and WEC3 & WEC7 (c).

Finally, the results of Figs. 6-7 demonstrate clearly that the presence of the wall, irrespectively of the distance of the array from this boundary, affects significantly the heave exciting forces of all the WECs at $0.01 \leq k_0b \leq 1.0$, since in this wave number range for both c/b values examined, F_Z does not show the continuous smooth decrease as in the case of the isolated array.

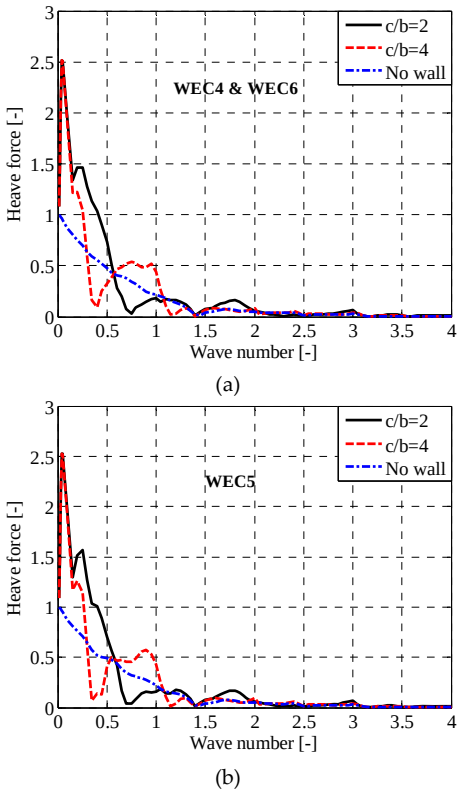

Fig. 7. Effect of c/b on heave force, F_Z, applied on WEC4 & WEC6 (a) and WEC5 (b).

C. *Effect of WECs-wall distance on the heave response*

The effect of the WECs-wall distance on the WECs' heave response is shown in Figs. 8-9, where the variation of RAO_3 for all the WECs of the array as a function of k_0b is presented for both $c/b = 2$ and 4, as well as for the isolated array.

In the case of $c/b = 4$, the variation of RAO_3 for each WEC is characterized by the existence of two distinctive peaks. The first one is observed at $k_0b = 0.05$ and it is related to the relevant rapid increase of the heave exciting forces (Figs. 6-7), while the second one occurs at $k_0b = 0.65$ and it is attributed to the occurrence of resonance. Moreover, the variation pattern of RAO_3 exhibits a distinctive local minimum at k_0b~0.4, as a result of the rapid decrease of F_Z at $0.05 < k_0b < 0.4$. By decreasing c/b to the value of 2, significant differences are introduced in the variation pattern and the values of RAO_3 at $0.05 < k_0b \leq 1.0$, related to the different variation of the heave exciting forces. (Figs. 6-7). Specifically, after obtaining its peak value at $k_0b = 0.05$, RAO_3 shows a general decreasing trend, with a quite irregular variation pattern (existence of multiple local minima and maxima) up to $k_0b = 0.5$. Moreover, no amplification of RAO_3 due to resonance occurs and the heave response exhibits a characteristic local minimum at $k_0b = 0.75$. The latter two features are attributed to the continuous decrease of F_Z at $0.5 < k_0b \leq 0.75$ and its minimization at $k_0b = 0.75$ (Figs. 6-7). All the above lead in turn to a great reduction of RAO_3 for $c/b = 2$ at $0.5 < k_0b < 1.0$ compared to $c/b = 4$, while the opposite holds true at $0.2 < k_0b < 0.5$.

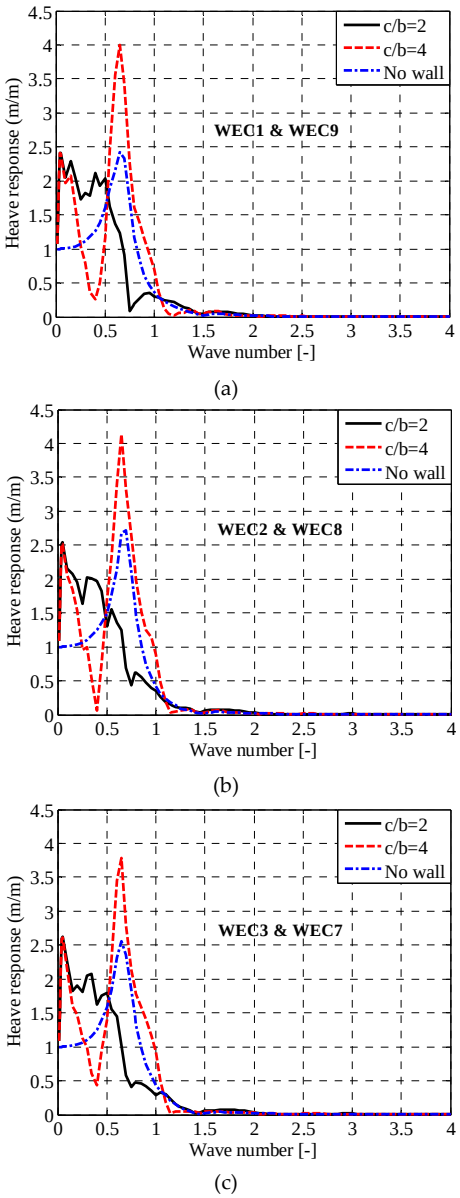

Fig. 8. Effect of c/b on heave response, RAO_3, of WEC1 & WEC9 (a), WEC2 & WEC8 (b) and WEC3 & WEC7 (c).

Compared to the isolated array, the results of Figs. 8-9 demonstrate that the presence of the wall, has a significant impact on RAO_3 of all the WECs at $0.01 \leq k_0b < 1.0$. Specifically, when the array is placed in front of the wall at a small distance from it ($c/b = 2$), the WECs' heave response becomes larger at $0.01 \leq k_0b < 0.5$, while a great reduction of RAO_3 occurs at $0.5 < k_0b < 1.0$. On the other hand, by increasing the distance of the array from the wall ($c/b = 4$), RAO_3 values, compared to the isolated array, increase significantly at $0.01 \leq k_0b < 0.3$ and in the k_0b range, where resonance phenomena occur, while the opposite holds true at $0.3 \leq k_0b < 0.5$.

D. *Effect of WECs-wall distance on the absorbed power and q_{mod}*

With regard to the absorbed power, Fig. 10 shows the variation of p_j, $j = 1, \ldots, 9$, absorbed by each WEC (12) as a function of k_0b for $c/b = 2$, $c/b = 4$ and for the isolated array. In the latter case (Fig. 10c), p_j, $j = 1, \ldots, 9$, varies smoothly and obtains peak values at $0.6 < k_0b < 0.75$. Analogous behaviour is observed for $c/b = 4$ (Fig. 10b); however, the presence of the wall boundary leads to larger peak values of the WECs' absorbed power. Compared to both the isolated array and $c/b = 4$, the placement of the WECs closer to the wall ($c/b = 2$, Fig. 10a) leads to a great reduction of the WECs' absorbed power global maxima, which, additionally, are shifted at smaller k_0b values ($0.3 < k_0b < 0.6$). Moreover, for $c/b = 2$, p_j, $j = 1, \ldots, 9$, exhibit a quite irregular pattern, with multiple peaks and minima at $0.1 \leq k_0b < 0.6$. It is, finally, noted that, for a given examined case, small differences in the power absorbed by the WECs are observed, bounded at $0.3 < k_0b < 0.6$ for $c/b = 2$ and at $0.6 < k_0b < 0.8$ for $c/b = 4$ and for the isolated array. All the above are in absolute accordance with the results of Figs. 8-9.

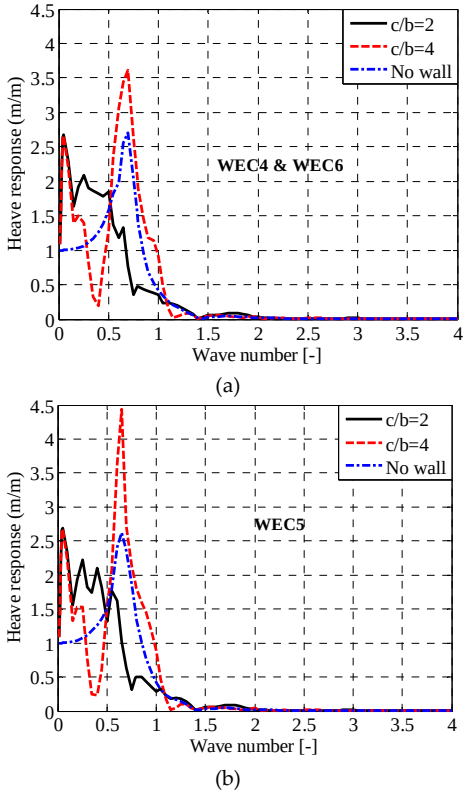

Fig. 9. Effect of c/b on heave response, RAO_3, of WEC4 & WEC6 (a) and WEC5 (b).

The effect of c/b on the power absorbed by the whole array is shown in Fig. 11a, where p (11) is plotted as a function of k_0b for all c/b values examined, as well as for the case of the isolated array. In the absence of the wall, significant amount of power is absorbed at $0.5 < k_0b < 1.0$. The same holds for $c/b = 4$; however, the existence of the wall affects positively the power absorption of the array leading to a great increase of p. Contrary to the above cases, the placement of the array close to the wall boundary ($c/b = 2$) leads to non-zero values of p at smaller k_0b values (i.e., at $0.1 < k_0b < 0.7$). Moreover, it results to a significant reduction of p compared to both $c/b = 4$ and the isolated array at $0.5 < k_0b < 1.0$, while the opposite holds true at $0.2 < k_0b < 0.5$.

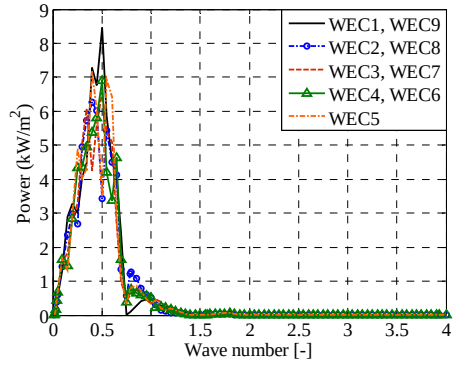

(a)

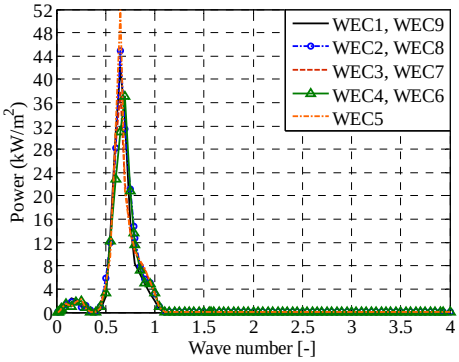

(b)

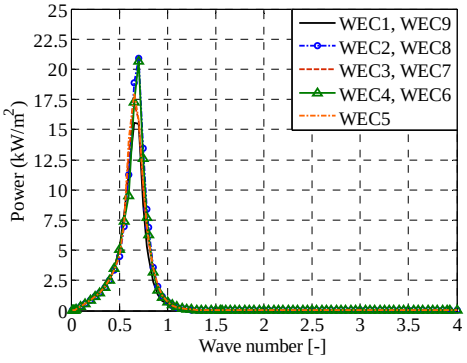

(c)

Fig. 10. Variation of $p_i, i = 1, \ldots, 9$, as a function of $k_0 b$ for $c/b = 2$ (a), $c/b = 4$ (b) and for the isolated array (c).

Finally, the effect of c/b on q_{mod} calculated for the whole array (Equation 13 with $N = 9$) is presented in Fig. 11b. For all examined c/b values intense interaction effects ($q_{mod} \neq 0$) occur at $0.01 < k_0 b < 1.0$. For $c/b = 4$, the WECs' hydrodynamic interactions in the presence of the wall have a significant positive effect ($q_{mod} > 0$) on the array's absorbed power at $0.5 < k_0 b < 1.0$, while the opposite holds true for $0.3 < k_0 b < 0.5$ ($q_{mod} < 0$). It is emphasized that the former constructive interactions are enhanced compared to the case of the isolated array. Contrary to $c/b = 4$ and the isolated array, by placing the array close to wall ($c/b = 2$), intense destructive interactions between the WECs occur at $0.5 < k_0 b < 1.0$ ($q_{mod} < 0$), while, the positive values of q_{mod} at $0.1 < k_0 b < 0.5$ illustrate the existence of constructive interactions at smaller wave numbers. All the above are in absolute accordance with the results presented previously in this section.

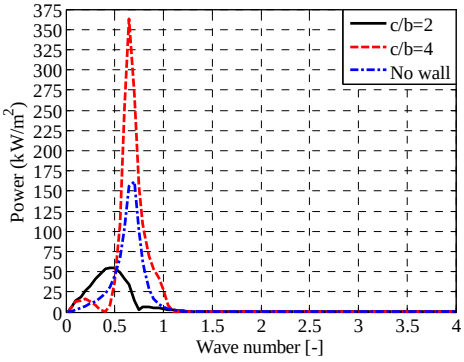

(a)

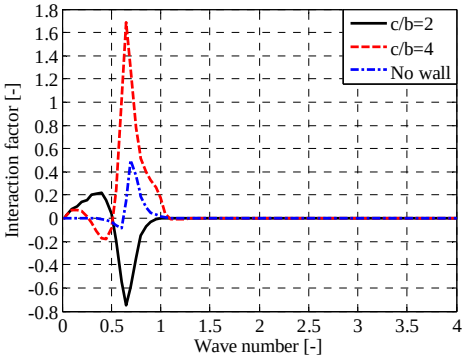

(b)

Fig. 11. Effect of c/b on total power, p, (a) and on q_{mod} (b).

V. CONCLUSIONS

In this paper, the hydrodynamic performance (hydrodynamic behaviour and power absorption) of a linear array of nine, free-floating heaving WECs placed in front of a bottom-mounted, finite–length, vertical wall of negligible thickness is investigated numerically in the frequency domain under the action of perpendicular regular waves. Emphasis is given on the effect of the array's distance from the wall (c/b) on the physical quantities describing the hydrodynamic performance of the array. Moreover, the limitations of the widely used method of images along with the assumption of a "pure" wave reflecting wall on the calculation of the WECs' exciting forces are examined and discussed. The main conclusions of the present investigation are:

• The infinite wall assumption leads to an under-estimation of the WECs' heave exciting forces at $k_0 b < 0.1$, even when a lengthy wall (with large outer WEC's centre–to–wall's edge distances), as in this paper, is taken into account. Thus, it shows limitations regarding the accurate estimation of the aforementioned physical quantities at quite small wave numbers.

• For the finite l_w case examined here, the infinite wall assumption does not have a significant effect on the WECs' surge and sway forces. Nevertheless, a careful use of the method of images is recommended, since differences between finite- and infinite-length wall cases do exist.

• The increase of c/b leads to a more intense variation of the WECs' surge and sway exciting forces. Contrary to the isolated array, the presence of the vertical bottom–

mounted, finite–length boundary in the leeward side of the WECs, irrespectively of their distance from it, introduces a continuous alternation of local maxima and minima in the variation pattern of the WECs' sway exciting forces.

• Regarding heave exciting forces, the presence of the wall, irrespectively of the WECs' distance from it, leads, contrary to the isolated array, to the existence of F_Z global maxima at $k_0b \neq 0.01$ with values larger than 1.0. Moreover, F_Z exhibits a distinctive local minimum at $0.2 \leq k_0b < 1.0$. At this wave number range, the change of c/b affects also the WECs' heave exciting forces. The most pronounced effect is the shift of the aforementioned F_Z local minimum from $k_0b{\sim}0.35$ to $k_0b{\sim}0.75$ by decreasing c/b, i.e., within the wave number range, where heave resonance phenomena occur.

• The change of c/b introduces significant differences in the variation pattern and the values of the WECs' heave response at $0.05 < k_0b \leq 1.0$ related to the different variation of the heave exciting forces. By decreasing c/b, no amplification of RAO_3 due to resonance occurs and a great reduction of $RA0_3$ is observed in the corresponding k_0b range ($0.5 < k_0b < 1.0$). However, for $c/b = 2$ $RA0_3$ exhibits larger values at small wave numbers ($0.2 < k_0b < 0.5$). Compared to the isolated array, the presence of the wall, has a significant impact on RAO_3 for all the WECs up to $k_0b = 1.0$.

• The placement of the array at a large distance from the wall ($c/b = 4$), enhances constructive interactions among the WECs at $0.5 < k_0b < 1.0$ compared to both $c/b = 2$ and the isolated array. Therefore, the power absorption of the array at this wave number range is increased. By decreasing the WECs' distance from the wall, the WECs hydrodynamic interactions have a positive effect on the array's absorbed power at smaller k_0b values, leading, therefore, to an enhanced power absorption at $0.1 < k_0b < 0.5$ compared to the rest examined cases.

The present investigation can be further extended in order to examine the effect of other characteristic parameters (e.g., length of the wall, PTO characteristics, wave directionality etc.) on the hydrodynamic performance of the array under the action of both regular and irregular waves.

REFERENCES

[1] D. Magagna and A. Uihlein, "Ocean energy development in Europe: Current status and future perspectives," *Int. J. Mar. Energy*, vol. 11, 2015, pp. 84–104. DOI: 10.1016/j.ijome.2015.05.001, [Online].

[2] A. F. de O Falcão, "Wave energy utilization: A Review of the technologies," *Renew. Sust. Energ. Rev.*, vol. 14, no. 3, pp. 899–918, 2010. DOI: 10.1016/j.rser.2009.11.003, [Online].

[3] D. Vicinanza, L. Margheritini, J. P. Kofoed and M. Buccino, "The SSG wave energy converter: Performance, status and recent developments", *Energies*, vol. 5, pp. 193-226, 2012. DOI: 10.3390/en5020193, [Online].

[4] M. A. Mustapa, O. B. Yaakob, Y. M. Ahmed, C.-K. Rheem, K. K. Koh, and F. A. Adnan, "Wave energy device and breakwater integration: A review", *Renew. Sust. Energ. Rev.*, vol. 77, pp. 43–58, 2017. DOI: 10.1016/j.rser.2017.03.110, [Online].

[5] S. Zheng and Y. Zhang, "Wave diffraction from a truncated cylinder in front of a vertical wall," *Ocean Eng.*, vol. 104, pp. 329–343, 2015. DOI: 10.1016/j.oceaneng.2015.04.065, [Online].

[6] S. Zheng and Y. Zhang, "Wave radiation from a truncated cylinder in front of a vertical wall," *Ocean Eng.*, vol. 111, pp. 602–614, 2016. DOI: 10.1016/j.oceaneng.2015.11.024, [Online].

[7] J. Schay, J. Bhattacharjee and C. G. Soares, "Numerical modelling of a heaving point absorber in front of a vertical wall," *in 32nd International Conference on Ocean, Offshore and Arctic Engineering*, 2013, vol. 8, Paper No. OMAE2013-11491.

[8] J. Falnes and J. Hals, "Heaving buoys, point absorbers and arrays," *Phil. Trans. R. Soc. A*, vol. 370, pp. 246–277, 2012. DOI: 10.1098/rsta.2011.0249, [Online].

[9] P. McIver and R. Porter, "The motion of a freely floating cylinder in the presence of a wall and the approximation of resonances," *J. Fluid Mech.*, vol. 795, pp. 581-610, 2016. DOI: 10.1017/jfm.2016.201, [Online].

[10] P. McIver and D. V. Evans, "An approximate theory for the performance of a number of wave-energy devices set into a reflecting wall", *Appl. Ocean Res.*, vol. 10, no. 2, pp. 58–65, 1988. DOI: 10.1016/S0141-1187(88)80032-4, [Online].

[11] S. A. Mavrakos, G. M. Katsaounis, K. Nielsen and G. Lemonis, "Numerical performance investigation of an array of heaving power converters in front of a vertical breakwater," in *14th International Offshore and Polar Engineering Conference*, 2004, vol. 1, pp. 238-245.

[12] X. Zhao, D. Ning, C. Zhang, Y. Liu and H. Kang, "Analytical study on an oscillating buoy wave energy converter integrated into a fixed box-type breakwater", *Math. Probl. Eng.*, vol. 2017, article ID 3960401, 2017. DOI: 10.1155/2017/3960401, [Online].

[13] D. Z.Ning, X. L. Zhao, L. F.Chen and M. Zhao, "Hydrodynamic performance of an array of wave energy converters integrated with a pontoon-type breakwater", *Energies*, vol. 11, paper no. 685, 2018. DOI: 10.3390/en11030685, [Online].

[14] I. K. Chatjigeorgiou, "Water wave trapping in a long array of bottomless circular cylinders," *Wave Motion*, vol. 83, pp. 25–48, 2018. DOI: 0.1016/j.wavemoti.2018.08.003, [Online].

[15] I. K. Chatjigeorgiou, K. Chatziioannou and T. Mazarakos, "Near trapped modes in a long array of truncated circular cylinders," *J. Waterw. Port Coast. Ocean Eng.*, vol. 145, no. 1, 2019. DOI: 10.1061/(ASCE)WW.1943-5460.0000495, [Online].

[16] C.H. Lee, "WAMIT theory manual," Department of Ocean Engineering, MIT. Cambridge, Massachusetts, USA. MIT Report 95-2, October 1995. [Online] Available: https://www.wamit.com/Publications/tmanual.pdf

[17] C.H. Lee and J.N. Newman, "Computation of wave effects using the panel method," in *Numerical Models in Fluid-Structure Interaction*, S. Chakrabarti ed. Southampton, UK, WIT Press, 2005, ch. 42, pp. 211-251.

[18] A. Babarit, "Impact of long separating distances on the energy production of two interacting wave energy converters," *Ocean Engin.*, vol. 37, no. 8-9, pp. 718–729, 2010. DOI: 10.1016/j.oceaneng.2010.02.002, [Online].

[19] B. Bogarino , A. Babarit and P. Ferrant, "Impact of wave interactions effects on energy absorption in large arrays of wave energy converters," *Ocean Engin.*, vol. 41, pp. 79–88, 2012. DOI: 10.1016/j.oceaneng.2011.12.025, [Online].

[20] J. Falnes, Ocean Waves and Oscillating Systems: Linear Interactions Including Wave-Energy Extraction. Cambridge: Cambridge University Press, 2002.